Pertanika J. Trop. Agric. Sci. 48 (1): 91 - 116 (2025)

PERTANIKA JOURNALS

TROPICAL AGRICULTURAL SCIENCE

Journal homepage: http://www.pertanika.upm.edu.my/

Nanoemulsion and Topical Cream for Delivery of Tocotrienol-rich fraction, Ascorbyl Tetraisopalmitate, and Carotenes: Formulation and *in vitro* Release

Yee-Lin Gan[1], Chin Ping Tan[2], Cheah Yoke Kqueen[3], Hidayah Ariffin[1,4], Helmi Wasoh[1] and Oi Ming Lai[1,5,6]*

[1]*Department of Bioprocess Technology, Faculty of Biotechnology and Biomolecular Sciences, Universiti Putra Malaysia, Serdang, Selangor, Malaysia*
[2]*Department of Food Technology, Faculty of Food Science and Technology, Universiti Putra Malaysia, Serdang, Selangor, Malaysia*
[3]*Department of Biomedical Sciences, Faculty of Medicine and Health Sciences, Universiti Putra Malaysia, Serdang, Selangor, Malaysia*
[4]*Laboratory of Biopolymer and Derivatives, Institute of Tropical Forestry and Forest Products, Universiti Putra Malaysia, Serdang, Selangor, Malaysia*
[5]*International Joint Laboratory on Plant Oils Processing and Safety, UPM-Jinan University China, Institute of Bioscience, Universiti Putra Malaysia, Serdang, Selangor, Malaysia*
[6]*Natural Product and Medicine Research, Institute of Bioscience, Universiti Putra Malaysia, Serdang, Selangor, Malaysia*

ABSTRACT

Objectives of this study were to encapsulate tocotrienol-rich fraction (TRF), ascorbyl tetraisopalmitate (AT) and carotenes into nanoemulsion, incorporate the formulated nanoemulsion into moisturizer cream, and characterize the formulated nanoemulsion and cream. A stepwise factorial design methodology was used to screen the nanoemulsion's ingredients and preparation parameters. With mean droplet size, polydispersity index (PDI), creaming index (CI) and irritational potential as evaluation criteria, the ideal nanoemulsion formulation comprised deionized water, red palm oil (RPO) and Kolliphor® EL in a ratio of 20.00:6.25:73.75, fabricated using a high-shear mixer at 7000 rpm and 45°C for 10 min followed by a high-pressure homogenizer at 750 bars for five cycles. The nanoemulsion's mean droplet size and PDI were 121.5 ± 1.8 nm and 0.178 ± 0.010, respectively. The cream formulation was then screened using a factorial experiment that considered lipid and emulsifier concentrations. The optimal cream formulation contained deionized water, formulated nanoemulsion, petrolatum, mineral oil, glycerol, emulsifying wax and carbomer 940

ARTICLE INFO

Article history:
Received: 23 April 2024
Accepted: 15 July 2024
Published: 28 January 2025

DOI: https://doi.org/10.47836/pjtas.48.1.06

E-mail addresses:
yeelingan@gmail.com (Yee- Lin Gan)
tancp@upm.edu.my (Chin Ping Tan)
ykcheah@upm.edu.my (Cheah Yoke Kqueen)
hidayah@upm.edu.my (Hidayah Ariffin)
helmi_wmi@upm.edu.my (Helmi Wasoh)
omlai@upm.edu.my (Oi Ming Lai)
* Corresponding author

ISSN: 1511-3701
e-ISSN: 2231-8542

in a ratio of 66.8:10.0:7.5:7.5:5.0:3.0:0.2, showing the preferred shear-thinning behavior, excellent physical stability and high conclusiveness. The formulated cream exhibited Korsmeyer-Peppas and Weibull release kinetic mechanisms during the in vitro release. This study showed that the developed formulations were suitable for the topical delivery system for TRF, AT and carotenes.

Keywords: Ascorbyl tetraisopalmitate, atopic dermatitis, carotenes, moisturizer cream, nanoemulsion, tocotrienol-rich fraction

INTRODUCTION

Atopic dermatitis (AD) is a common chronic skin disorder associated with a relapsing-remitting inflammatory condition, persistent pruritus and xerosis. The interaction of epidermal dysfunction and immune dysregulation is a key pathophysiological mechanism of AD (Williamson et al., 2020). Though non-life threatening, AD symptoms have considerably impaired the quality of life of patients and caregivers (Laughter et al., 2021). No curable medicine is available, and current AD management mainly focuses on flare prevention and symptom relief to enable patients to attain satisfying functional life status. It involves the daily application of moisturizer to restore and maintain skin barrier function, thus reducing the number of skin flares during the remitting period (Weber et al., 2015; Zuuren et al., 2017). During the relapsing period, topical corticosteroids or calcineurin inhibitors are twice-daily applied as the first-line treatment. However, concerns have been raised as topical corticosteroids and calcineurin inhibitors are associated with considerable side effects. Concerns regarding the adverse side effects have hindered the application of topical drugs. To minimize topical corticosteroids or calcineurin inhibitors, efforts have been made to discover and incorporate ingredients that possess skin repairment and anti-inflammatory properties into the moisturizer (Hebert et al., 2020).

It is evident that AD patients are characterized by lower levels of antioxidants and increased oxidative stress compared to healthy controls (Amin et al., 2015; Leveque et al., 2003; Sivaranjani et al., 2013). Disrupted antioxidant defense promotes dysregulation of skin homeostasis and immune response, encouraging AD development (Ji & Li, 2016). Thus, reinforcing the antioxidant systems by increasing the skin's antioxidant capacity is a potential drug-sparing strategy for managing AD. Vitamin E, vitamin C, and carotenes are the predominant exogenous antioxidants in the skin. Previous studies reported that vitamin E can improve epidermal function by upregulating the expression of epidermal differentiation enzymes and proteins, increasing ceramide production, and reducing transepidermal water loss (TEWL) (De Pascale et al., 2006; Kato & Takahashi, 2012; Parish et al., 2005). As well, vitamin E reduced inflammatory conditions and ameliorated AD symptoms in sensitized animals and AD patients (Babaye-Nazhad et al., 2013; Hayashi et al., 2012; Jaffary et al., 2015; Javanbakht et al., 2011; Kapun et al., 2014; Tsuduki et al., 2013). Similarly, literature also has demonstrated that vitamin C promoted keratinocyte differentiation,

reduced TEWL, and improved inflammatory status and AD symptoms in sensitized animals (Pasonen-Seppänen et al., 2001; Savini et al., 2002; Parish et al., 2005; Kim et al., 2015; Lee et al., 2017). Meanwhile, findings demonstrated that β-carotene significantly improved the scratching behavior, skin moisture level and inflammatory status in sensitized animals (Hiragun et al., 2016; Kake et al., 2019; Sakai et al., 2011; Sato et al., 2004)

Considering that topical agents are the mainstays for localized AD treatment and the adsorption and biodistribution of exogenous antioxidants following oral administration exhibit isomeric and regional variations that affect the delivery of antioxidants to the targeted skin sites, topical delivery of these antioxidants is thus recommended (Hemrajani et al., 2022; Myriam et al., 2006; Packer et al., 2001). However, the limited solubility and poor skin penetration of antioxidants hinder their practical application when delivered topically, consequently diminishing their efficacy. Many delivery systems have been developed to overcome these issues. Amongst the delivery systems, nanoemulsion emerges as a promising approach. Pertaining to the nano-size droplets (20–200 nm), nanoemulsion can improve solubilities, increase thermodynamic activities, favor partitioning and promote skin penetration of the encapsulated compounds (Hemrajani et al., 2022). However, the rheology characteristics of watery nanoemulsion, which have low viscosity, limit their feasibility in the practical topical application (Chellapa et al., 2015). Fortunately, nanoemulsion can be further incorporated into different formulations, such as creams and gels, to solve the problem.

In light of the information above, the main objectives of this study were to develop an oil-in-water nanoemulsion loaded with vitamin E (tocotrienol-rich fraction [TRF]), vitamin C (AT) and carotenes using high-pressure homogenization by studying the influence of ingredients and preparation process conditions. The nanoemulsion with a small mean droplet size, lowest polydispersity index (PDI), zero creaming index (CI) and lowest irritational potential was subsequently formulated into moisturizer cream by considering the effect of the cream's ingredients. Physical stability, spreadability, rheological behavior, and occlusion factors were used as evaluation parameters for the cream formulation selection. Finally, the behavior of the selected nanoemulsion and moisturizer cream formulations was determined.

MATERIALS AND METHODS

Materials

Rice bran, sunflower, olive, canola and red palm oils were purchased from local markets. TRF, AT and carotenes were procured from Sime Darby Sdn. Bhd. (Selangor, Malaysia), Nikko Chemicals Co. Ltd. (Tokyo, Japan), and Super Vitamins Sdn. Bhd. (Johor, Malaysia), respectively. Tween 80 and Tween 20 were supplied by Thermo Fisher Scientific Inc. (Massachusetts, USA) and Merck KGaA (Darmstadt, Germany), respectively. Kolliphor® EL and Tween 85 were obtained from Sigma-Aldrich Corporation (Missouri, USA). Mineral

oil, petrolatum, emulsifying wax, and carbomer 940 were acquired from Spectrum Chemical Manufacturing Corporation (New Jersey, USA). Glycerol and sodium hydroxide were supplied by Fisher Scientific UK Ltd. (Leicestershire, UK). The water was purified and deionized using the Millipore system (Millipore GmbH, Darmstadt, Germany). All other chemicals and solvents were either in analytical or high-performance liquid chromatography (HPLC) grade.

Formulation of Oil-in-Water Nanoemulsion

Screening of Oils

For the solubility study of carotenes, an excess amount of carotenes was added to 5 g of oil (rice bran, sunflower, olive, canola and red palm oils) in a tube, blanketed with nitrogen, sonicated for 30 min (Model Powersonic 520, Hwashin Tech Co., Ltd., Seoul, Korea, 40 kHz), then shaken at 150 rpm and 25°C for 72 hr in an orbital shaking incubator (Model LSI-3016A, Daihan Labtech Co., Ltd., Gyeonggi-do, Korea) (Roohinejad et al., 2015). The resulting samples were centrifuged at 18000 × *g* for 15 min to remove undissolved carotenes. The supernatant oil fraction was filtered through 0.45 µm polytetrafluoroethylene membrane filters, and the concentration of dissolved carotenes was quantified using HPLC.

To determine the thermal stability of total antioxidants, 5% w/w TRF, 5% w/w AT and 0.5% w/w carotenes were dissolved in each oil type via sonication for 30 min. One gram of the sample was heated at 45°C, 60°C and 75°C in a water bath for 1 h, cooled to room temperature, and the retained number of antioxidants was determined using HPLC. The oil that provides greater thermal stability and higher solubility was selected for subsequent experiments**.**

Screening of Coarse Emulsion Formation Preparation Process Conditions

The 20% w/w oil phase (1% w/w TRF, 1% w/w AT and 0.1% w/w carotenes at final concentration) was mixed with 80% w/w aqueous phase (deionized water with 5% w/w Tween 80 at final concentration), using a high-shear mixer (Model L4RT, Silverson Machines, Inc., USA). The processing conditions evaluated were homogenization speed (5000 to 9000 rpm), time (1 min to 10 min) and temperature (30°C to 60°C). The prepared coarse emulsions' mean droplet size, PDI and CI were evaluated. The preparation process conditions producing a coarse emulsion with the lowest mean droplet size, PDI and CI, were used for subsequent experiments.

Screening of Nanoemulsion Formation Preparation Process Conditions

The coarse emulsions were prepared by mixing 20% w/w oil phase (1% w/w TRF, 1% w/w AT and 0.1% w/w carotenes at final concentration) and the 80% w/w aqueous phase

(5% w/w Tween 80 at final concentration), using a high-shear mixer at 7000 rpm and 45°C for 10 min. The temperature was adjusted during preparation in the incubator. The coarse emulsions were immediately placed into a high-pressure homogenizer (Model Panda PLUS 2000, GEA Niro Soavi, Italy). The processing conditions studied were homogenization pressure (250 to 1250 bar) and cycle (one to eight). The prepared nanoemulsion were examined for their mean droplet size, PDI and CI. The preparation process conditions that can produce nanoemulsion with small droplet size (100–200 nm), PDI <0.200 and zero CI were used for the following experiments.

Screening of Types of Surfactants and Surfactant-to-Oil Ratio

The non-ionic surfactants studied in this experiment were Tween 85 [Hydrophilic-Lipophilic Balance (HLB):11], Kolliphor® EL (HLB:12–14), Tween 80 (HLB:15) and Tween 20 (HLB:16.7) at the surfactant-to-oil ratio of 1:8, 1.5:8, 2:8, 2.5:8, 3:8, 3.5:8 and 4:8. The coarse emulsions were prepared by mixing 20% w/w oil phase (1% w/w TRF, 1% w/w AT and 0.1% w/w carotenes at final concentration) with aqueous phase that containing the targeted type and concentration of surfactants, using a high-shear mixer at 7000 rpm and 45°C for 10 min. The coarse emulsions were rapidly processed using a high-pressure homogenizer at 750 bars for five cycles. Mean droplet size, PDI, CI and irritation potential were measured for each prepared nanoemulsion. The type of surfactant at a surfactant-to-oil ratio that can produce nanoemulsion with a mean droplet size between 100 to 200 nm, PDI <0.200, zero CI and lowest irritational potential was selected as the best formulation.

Evaluation of Coarse Emulsion and Nanoemulsion

Mean Droplet Size and PDI Evaluations

Each sample was diluted 10 times with deionized water to minimize the multiple scattering effects. The mean droplet size and PDI measurements were carried out at 25 ± 0.5°C using a dynamic light scattering instrument (Model Zetasizer Nano ZS, Malvern Instruments Ltd., UK), as previously described (Uluata et al., 2016). The mean droplet size is calculated using the photon correlation spectroscopy concept combined with cumulant methods and expressed as the *Z*-average droplet diameter. The PDI results were determined based on the volume versus droplet diameter profile. The refractive indices of the dispersed and continuous phases employed for the PDI calculation were 1.47 and 1.33, respectively.

CI Evaluation

The CI was determined using a previously described method (Uluata et al., 2016). Ten milliliters of each freshly prepared sample were transferred into new tubes and incubated for 24 hr at room temperature. The entire height of the samples (H_E) and the height of

the cream layer (H_C) were determined using a ruler, and the magnitude of creaming was calculated using Equation 1:

$$CI\ (\%) = H_C/H_E \times 100\% \quad [1]$$

Irritational Potential Evaluation

The irritational potential for each surfactant at the concentrations used in nanoemulsion preparation was determined using the erythrocytes cellular model and expressed as hemolysis percentage (Rocha-Filho et al., 2017). Human blood was collected in a vacutainer tube containing ethylenediaminetetraacetic acid, mixed well and centrifuged at 650 × *g* for 10 min. The supernatant was discarded, and the erythrocytes were resuspended in phosphate buffer saline (PBS) (pH 7.4). Next, the erythrocytes were washed three times using PBS in a volume ratio 4:1. In each washing step, the buffy coat (precipitated debris and serum proteins) in the upper phase was removed. The erythrocytes were resuspended in PBS to achieve 50% hematocrit in the final wash. Twenty-five microliters of erythrocyte suspension and 975 µL of the sample were then aliquoted into a tube and incubated in a water bath under 100 rpm shaking speed for 30 min at 37°C. Later, the intact and debris erythrocytes were removed via 10 min centrifugation at 650 × *g*. The hemoglobin released into the supernatant was analyzed spectrophotometrically at 540 nm against a corresponding blank sample. The percentage of hemolysis (H%) was calculated based on the released hemoglobin using Equation 2:

$$H\ (\%) = (A_S - A_{C1})/\ (A_{C2} - A_{C1}) \times 100 \quad [2]$$

Where A_S refers to the absorbance of the sample, A_{C1} refers to the absorbance of mechanical hemolysis (erythrocytes in a PBS solution; hemolysis happened due to sample preparation), and A_{C2} refers to the absorbance of 100% hemolysis (erythrocytes in deionized water).

Formulation of Moisturizer Creams

The aqueous phase was prepared by hydrating 0.2% w/w carbomer 940 and dissolving 5% w/w glycerol in deionized water (Table 1). The oil phase consisted of a 5 to 10% w/w mixture of mineral oil and petrolatum (ratio 1:1) and 1 to 5% w/w emulsifying wax mixed homogeneously (Table 1). Both phases were heated to 70°C using a water bath. The oil phase was then gradually added to the aqueous phase at a stirring speed of 500 rpm until the temperature dropped to 40°C. Then, 10% w/w of nanoemulsion was added and stirred at 200 rpm for 10 min. The pH value of the mixture was adjusted to 5.5 using 1 M sodium hydroxide to impart the thickening property of carbomer 940. The physically stable and semifluid-formulated cream with shear-thinning rheological behavior and the highest occlusion factor was selected for further analysis.

Table 1
Formulation of moisturizer creams

Formulation	Weight (% w/w)							
	Petrolatum	Mineral oil	Emulsifying wax	Glycerol	Nanoemulsion	Carbomer 940	Sodium hydroxide	Deionized water
TC01	2.5	2.5	1.0	5.0	10.0	0.2	qs	qs ad to 100
TC02	5.0	5.0	1.0	5.0	10.0	0.2	qs	qs ad to 100
TC03	7.5	7.5	1.0	5.0	10.0	0.2	qs	qs ad to 100
TC04	10.0	10.0	1.0	5.0	10.0	0.2	qs	qs ad to 100
TC05	2.5	2.5	2.0	5.0	10.0	0.2	qs	qs ad to 100
TC06	5.0	5.0	2.0	5.0	10.0	0.2	qs	qs ad to 100
TC07	7.5	7.5	2.0	5.0	10.0	0.2	qs	qs ad to 100
TC08	10.0	10.0	2.0	5.0	10.0	0.2	qs	qs ad to 100
TC09	2.5	2.5	3.0	5.0	10.0	0.2	qs	qs ad to 100
TC10	5.0	5.0	3.0	5.0	10.0	0.2	qs	qs ad to 100
TC11	7.5	7.5	3.0	5.0	10.0	0.2	qs	qs ad to 100
TC12	10.0	10.0	3.0	5.0	10.0	0.2	qs	qs ad to 100
TC13	2.5	2.5	4.0	5.0	10.0	0.2	qs	qs ad to 100
TC14	5.0	5.0	4.0	5.0	10.0	0.2	qs	qs ad to 100
TC15	7.5	7.5	4.0	5.0	10.0	0.2	qs	qs ad to 100
TC16	10.0	10.0	4.0	5.0	10.0	0.2	qs	qs ad to 100
TC17	2.5	2.5	5.0	5.0	10.0	0.2	qs	qs ad to 100
TC18	5.0	5.0	5.0	5.0	10.0	0.2	qs	qs ad to 100
TC19	7.5	7.5	5.0	5.0	10.0	0.2	qs	qs ad to 100
TC20	10.0	10.0	5.0	5.0	10.0	0.2	qs	qs ad to 100

Note. qs = Quantity sufficient; qs ad = Quantity sufficient to make

Evaluation of Moisturizer Creams

Physical Stability and Spreadability Evaluations

Freshly prepared creams (10g) were stored at 25°C and 40°C for 24 hr and subjected to centrifugation at 3000 rpm for 30 min (Dantas et al., 2016). The macroscopic observation was then performed to determine the presence of physical instability (creaming, cracking, phase inversion, bleeding or oiling off).

The spreadability of creams was determined using the parallel plate method (Oladimeji et al., 2015). Cream samples, prepared 48 hr prior, weighing 1 ± 0.01 g, were positioned at the center of a circular glass plate (diameter: 15 cm). A second glass plate (weighing 125 ± 1 g) was then placed atop the cream. The spreading diameter was measured after 1

min, enabling classification into three categories based on diameter: semistiff cream (25 mm < ∅ ≤ 50 mm), semifluid cream (50 mm < ∅ ≤ 70 mm), and fluid cream (∅ > 70 mm). Semifluid formulations demonstrating physical stability were chosen for subsequent evaluation of rheological behavior and in vitro occlusive properties.

Rheological Behaviors Evaluation

The rheological behaviors of cream were evaluated using a HAAKE RheoStress 6000 rheometer (Thermo Fisher Scientific Inc., USA) equipped with a Peltier system and 35 mm stainless steel serrated parallel plate. About 0.5 g of cream sample was put on the lower plate for each evaluation. The lower plate was slowly raised to the preset trimming gap of 0.55 mm. After removing the excess cream, the lower plate was lifted to the measurement geometry gap of 0.5 mm. The sample was equilibrated at 25 ± 0.1°C for 5 min. The flow property of the cream was characterized using the steady-state-flow method. The shear rate over a 0.01 to 100 $^{s-1}$ range was programmed in a logarithmic ramp mode in 3 min (Siska et al., 2019). The recorded results were plotted in a graph and fitted into the mathematical model of Power Law to calculate the flow behavior and consistency indices.

In vitro Occlusive Evaluation

A 50 ml beaker was filled with 20 ml of water, then enclosed with cellulose acetate filter paper (0.2 µm, Sartorius AG, Goettingen, Germany) (Swarnavalli et al., 2016). A 200mg cream sample was applied and spread evenly on the filter surface. The beaker without cream application on the filter served as a control. All the prepped beakers were incubated at 32°C and 50°C at 55% Relative Humidity (RH) for 24 h. The prepped beakers were weighed to determine the water loss through the filter due to evaporation. The occlusion factor for each sample, F, was then calculated using Equation 3:

$$F\ (\%) = (A - B)/A \times 100\% \quad [3]$$

Where A refers to the water loss without cream applied on the filter (control), and B represents the water loss with the cream applied on the filter.

Characterization of the Selected Nanoemulsion and Moisturizer Cream Formulations

Morphological Study

The selected nanoemulsion formulation was diluted ten times with deionized water. A drop of diluted sample was deposited on a carbon film-covered 400 mesh copper grid. Excess nanoemulsion was blotted with filter paper from the copper grid to produce a thin-film specimen. The specimen was negatively stained with 1% w/w uranyl acetate, air-dried

and examined under a Jem-2100F field emission electron microscope (Jeol Ltd., Tokyo, Japan), which operated at an accelerating voltage of 200 kV.

Morphology of the selected cream formulation was observed using an optical microscope (Model Olympus CX23, Olympus Corporation, Japan). The cream was applied, spread evenly onto a microscopic glass slide, and viewed under the microscope. The images were taken and processed using the ToupCam camera and ToupView software (ToupTek Photonics Co., Ltd., China).

In vitro Release

In vitro release profiles of antioxidants from nanoemulsion and moisturizer cream were investigated and compared to bulk oil using the Franz diffusion method (Jung et al., 2012). 0.45 µm cellulose acetate membrane (diameter: 25 mm) was presoaked in the receiver medium (PBS and ethanol in the ratio 1:1, pH 7.4) for 30 min, then mounted between the donor and receiver compartments of the Franz diffusion cell. The receiver chamber was then filled with receiver medium. The receiver fluid was continuously stirred with a magnetic stirrer at 500 rpm and 32 ± 0.5 °C. After equilibrating for 15 min, 1 g of sample was placed into the donor compartment and covered with parafilm. At predetermined intervals (1, 2, 3, 4, 5, 6, 8 and 12 h), 400 µL of samples were collected from the received chamber, and 400 µL of fresh receiver medium was refilled back. The samples were analyzed using HPLC. The cumulative number of antioxidants released per surface area of the membrane (µg cm^{-2}) was calculated using Equation 4 and plotted as a function of time (t):

$$Q = [C_nV + \sum_{i=1}^{n-1} CiS]/A \quad [4]$$

Where Q refers to the cumulative amount of antioxidants released per surface area of membrane (µg/cm^2), Cn denotes the concentration of antioxidants (µg/ml) determined at the nth sampling interval, V is the volume of individual Franz diffusion cell, $\sum_{i=1}^{n-1} Ci$ refers to the sum of concentrations of antioxidants (µg/ml) determined at sampling intervals 1 through n-1, S represents the volume of sampling aliquot (0.4 ml), and A is the surface area of Franz diffusion cell (2.27 cm^2).

The data were then fitted to the kinetic Equations 5 and 6:

Zero-order model (Salamanca et al., 2018):

$$Qt = Q_0 + k_{0t} \quad [5]$$

Where Qt is the percentage of the released antioxidants at time t, Q_0 represents the initial percentage of antioxidants in the receiver compartment (normally zero), k_0 denotes the rate constant of zero-order release kinetics, and t is the sampling time.

First-order model (Bruschi, 2015):

$$LogQt = LogQ0 + k1t/2.303 \quad [6]$$

Where Qt is the percentage of antioxidants that remained in the donor compartment at time t, Q0 represents the initial percentage of antioxidants in the donor compartment, k1 denotes the rate constant of first-order release kinetics, and t is the sampling time.

Higuchi model (Paarakh et al., 2018), Equation 7:

$$Q_t = k_H t^{1/2} \quad [7]$$

Where k_H represents the Higuchi dissolution constant, and t represents the sampling time.

Korsmeyer-Peppas model (Yarce et al., 2016), Equation 8:

$$Mt/M_\infty = k_r t^n \quad [8]$$

Where Mt is the percentage of the released antioxidants at time t, M_∞ represents the percentage of the released antioxidants at infinity time, kr denotes the release constant, t is the sampling time, and n is the diffusion exponent (related to the release mechanism).

Weibull model (Ye et al., 2019), Equation 9:

$$\ln[-\ln(1 - Qt)] = \ln(\propto) + \beta\ln t \quad [9]$$

Where $\propto$ represents the scale parameter that defines the timescale of the process, β denotes the curve shape factor, and t is the sampling time.

Based on the r^2 values and Akaike information criterion (AIC), the best model to describe the kinetics and mechanisms of antioxidants released was identified (Jahromi et al., 2020).

Statistical Analysis

All measurements were performed in triplicates and reported as mean value ± SD. The data were analyzed by one-way or two-way analysis of variance (ANOVA) using Minitab Statistical Software Release16 (Minitab, LLC., Pennsylvania, USA), followed by Tukey's post hoc test.

RESULTS AND DISCUSSION

Nanoemulsion Formulation

Influence of Oil Types on the Solubility of Carotenes and Thermal Stability of Antioxidants

Long-chain triacylglycerols, known as ripening inhibitors, were selected as the carrier oil for the current nanoemulsion formulation. Since TRF and AT used in this study were

in oil form, and carotenes are sparingly oil-soluble, the solubility of carotenes in various long-chain triacylglycerols was determined. Results showed that the solubility of carotenes was not significantly different ($p > 0.05$) among the tested long-chain triacylglycerols (Table 2). Further investigation was done to determine the thermal stability of total antioxidants dissolved in these long-chain triacylglycerols, considering heat generated during nanoemulsion preparation using high-pressure homogenization can degrade the antioxidants easily (Kruszewski et al., 2021). It was found that the retention efficiency of total antioxidants in red palm oil (RPO) was significantly higher than ($p < 0.05$) other oils, with no evidence of antioxidant degradation at 45°C (Table 2). Findings obtained following 1 hr heat treatment at 60°C showed that the retention efficiency in RPO was slightly lower than in rice bran oil. However, this difference did not reach statistical significance ($p > 0.05$) (Table 2). Current results show that RPO provided greater thermal stability to antioxidants and was chosen as the carrier oil for subsequent experiments.

Table 2
Solubility of carotenes and thermal stability of total antioxidants in different long-chain triacylglycerols

Oil	Rice bran	Olive	Canola	Sunflower	Red palm
	Solubility of carotenes (mg/g of oil)				
	43.13 ± 1.58^{a}	42.93 ± 1.59^{a}	44.68 ± 1.67^{a}	44.33 ± 1.74^{a}	44.81 ± 0.28^{a}
Temperature	**Total antioxidant retention (%) after 1 hr thermal treatment**				
45°C	97.22 ± 0.41^{a}	98.94 ± 0.28^{b}	97.21 ± 0.51^{a}	99.47 ± 0.27^{b}	100.96 ± 0.29^{c}
60°C	95.64 ± 0.75^{a}	98.65 ± 0.61^{b}	95.57 ± 0.66^{a}	95.20 ± 0.35^{a}	97.49 ± 0.63^{b}
75°C	93.97 ± 1.01^{a}	94.23 ± 0.86^{a}	91.32 ± 0.29^{b}	93.07 ± 0.45^{ab}	94.59 ± 0.65^{a}

Note. Different superscript alphabets a, b and c in the same row denote statistical significance ($p < 0.05$)

Process Conditions of High-speed Homogenization

Although coarse emulsion formation using high-speed homogenization is a preparatory step before nanoemulsion formation, it may affect the resulting nanoemulsion's mean droplet size and PDI (Galvão et al., 2018). This experiment used a high-shear mixer with a fixed workhead (emulsor screens) to prepare coarse emulsions. The effects of homogenization speed, time and temperature on coarse emulsion formation were evaluated. A significant inverse relation existed between homogenization time and mean droplet size of coarse emulsion when homogenization speed was kept constant (Table 3). A significant negative correlation was also found between the homogenization speed and mean droplet size when homogenization time was fixed at 1 min and 5 min. With 10 min of homogenization, the mean droplet size of coarse emulsion was significantly reduced when the homogenization speed increased from 5000 to 7000 rpm ($p < 0.05$); a further increment from 7000 to 9000 rpm did not reduce the mean droplet size. Synchronously, PDI and CI of coarse emulsion remained constant after 10 min of homogenization at speeds varying from 7000 to 9000 rpm (Table 3).

Hence, homogenization speed and time at 7000 rpm and 10 min were selected and applied in the screening experiment of homogenization temperature. When the homogenization temperature increased from 30°C to 60°C, the viscosity of emulsion phases decreased, and higher-intensity disruptive forces could be generated. Still, the coarse emulsion formed depicted no significant change ($p > 0.05$) in mean droplet size (Table 4). Previous studies (Jafari et al., 2008; Kuhn & Cunha, 2012; Peng et al., 2015; Qian & McClements, 2011) have reported that the mean droplet size of nanoemulsion is an equilibrium result of droplet disintegration and recoalescence during homogenization. At this point, surfactants absorb and cover the new interface of the small droplets formed before they collide to recoalesce. However, when the timescale of collision is shorter than the timescale of surfactant absorption, a high recoalescence rate increases the mean droplet size of nanoemulsion, implying the effects of overprocessing conditions; thus, when the temperature increases, the intensity of the disruptive forces increases with increasing viscosity. The intensity of disruptive forces generated and the time exposure greatly affect

Table 3
Effects of high-shear mixer's homogenization speed and time on the mean droplet size, PDI and CI of coarse emulsions

Homogenization speed (rpm)	Homogenization time (min)		
	1	5	10
	Mean droplet size (nm)		
5000	$7226.3 \pm 280.4^{A,a}$	$831.1 \pm 63.4^{B,a}$	$470.7 \pm 19.9^{C,a}$
6000	$4824.5 \pm 215.8^{A,b}$	$801.9 \pm 45.8^{B,a}$	$358.4 \pm 29.2^{C,b}$
7000	$1711.0 \pm 111.1^{A,c}$	$452.5 \pm 23.0^{B,b}$	$236.5 \pm 10.1^{C,c}$
8000	$1089.0 \pm 50.7^{A,d}$	$410.9 \pm 35.2^{B,bc}$	$235.2 \pm 11.4^{C,c}$
9000	$665.4 \pm 25.7^{A,e}$	$374.1 \pm 19.8^{B,c}$	$232.0 \pm 7.5^{C,c}$
	PDI		
5000	$0.229 \pm 0.041^{A,a}$	$0.229 \pm 0.041^{A,a}$	$0.229 \pm 0.041^{A,a}$
6000	$0.472 \pm 0.051^{A,b}$	$0.472 \pm 0.051^{A,b}$	$0.472 \pm 0.051^{A,b}$
7000	$1.000 \pm 0.000^{A,c}$	$1.000 \pm 0.000^{A,c}$	$1.000 \pm 0.000^{A,c}$
8000	$1.000 \pm 0.000^{A,c}$	$1.000 \pm 0.000^{A,c}$	$1.000 \pm 0.000^{A,c}$
9000	$1.000 \pm 0.000^{A,c}$	$1.000 \pm 0.000^{A,c}$	$1.000 \pm 0.000^{A,c}$
	CI (%)		
5000	$27.76 \pm 2.19^{A,a}$	$27.76 \pm 2.19^{A,a}$	$27.76 \pm 2.19^{A,a}$
6000	$24.12 \pm 0.74^{A,b}$	$24.12 \pm 0.74^{A,b}$	$24.12 \pm 0.74^{A,b}$
7000	$19.82 \pm 0.25^{A,c}$	$19.82 \pm 0.25^{A,c}$	$19.82 \pm 0.25^{A,c}$
8000	$19.43 \pm 0.48^{A,c}$	$19.43 \pm 0.48^{A,c}$	$19.43 \pm 0.48^{A,c}$
9000	$18.49 \pm 0.53^{A,c}$	$18.49 \pm 0.53^{A,c}$	$18.49 \pm 0.53^{A,c}$

Note. Different capital superscript alphabets A, B and C in the same row, while different small superscript alphabets a, b and c in the same column denote statistical significance ($p < 0.05$). PDI = polydispersity index; CI = creaming index

the emulsification efficiency, which may affect the droplet size. However, a considerable improvement in PDI and CI was detected when the processing temperature increased to 45°C, with no additional improvement observed at 60°C (Table 4). Considering these results, the process conditions at 7000 rpm and 45°C for 10 min were chosen to prepare coarse emulsion.

Table 4
Effects of high-speed homogenization processing temperature on the mean droplet size, PDI and creaming index of coarse emulsions

Processing temperature	**30°C**	**45°C**	**60°C**
Mean droplet size (nm)	263.6 ± 16.9^{a}	262.8 ± 4.7^{a}	262.8 ± 8.3^{a}
Polydispersity Index (PDI)	0.746 ± 0.016^{a}	0.725 ± 0.005^{b}	0.715 ± 0.011^{b}
Creaming index (%)	14.21 ± 0.80^{a}	11.95 ± 0.88^{b}	10.98 ± 0.55^{b}

Note. Different superscript alphabets a and b in the same row denote statistical significance ($p < 0.05$)

Influence of High-Pressure Homogenization's Process Conditions

Theoretically, when a coarse emulsion is subjected to high-pressure homogenization, the intensity of disruptive forces generated and the time exposure greatly affect the emulsification efficiency of the surfactant. Therefore, the influence of homogenization pressures and cycles on the formation of nanoemulsion was examined. Overall, nanoemulsion's mean droplet size and PDI decreased modestly with increasing homogenization pressures and cycles (Table 5). The presence of a creaming layer evidenced that a single homogenization cycle at all homogenization pressures could not produce a stable nanoemulsion (Table 5). At low pressures varied from 250 to 500 bar, nanoemulsion with small mean droplet size and PDI < 0.200 could not be generated (Table 5). At higher pressure (750 to 1250 bar), it was observed that the mean droplet size and PDI of nanoemulsion remained consistent from the 5^{th} to 8^{th} homogenization cycles. During the 5^{th} homogenization cycle, an increase in homogenization pressure from 750 to 1250 bar did not decrease mean droplet size and PDI. Since the mean droplet size and PDI did not reduce significantly after homogenization at 750 bars for five cycles, these settings were used throughout the following experiments to prepare nanoemulsion.

Influence of Types of Surfactants and Surfactant-to-Oil Ratio

Non-ionic surfactants that pose low skin irritation and safety issues are preferably used in dermatological products. In this study, the influence of four types of non-ionic surfactants (Tween 85, Kolliphor® EL, Tween 80 and Tween 20) at different surfactant-to-oil ratios on mean droplet size, PDI, CI and irritation potential was examined. All the tested surfactants at any surfactant-to-oil ratio formed a stable nanoemulsion with no creaming issue. When

Table 5
Effects of high-pressure homogenization pressures and cycles on the mean droplet size, CI and PDI of nanoemulsion

Cycle	Homogenization pressure (bar)				
	250	500	750	1000	1250
	Mean droplet size (nm)				
1	$219.7 \pm 1.5^{A,a}$	$184.4 \pm 4.6^{B,a}$	$166.4 \pm 1.6^{C,a}$	$157.2 \pm 0.7^{C,a}$	$163.6 \pm 9.1^{C,a}$
2	$197.6 \pm 2.0^{A,b}$	$170.9 \pm 0.3^{B,b}$	$152.2 \pm 1.9^{C,b}$	$143.0 \pm 0.9^{D,b}$	$147.0 \pm 7.7^{CD,b}$
3	$193.3 \pm 1.9^{A,bc}$	$165.3 \pm 0.2^{B,c}$	$144.5 \pm 2.6^{C,c}$	$137.7 \pm 1.4^{C,c}$	$142.3 \pm 7.9^{C,b}$
4	$190.4 \pm 1.4^{A,bcd}$	$159.8 \pm 0.6^{B,d}$	$138.1 \pm 3.9^{C,c}$	$134.4 \pm 0.8^{C,d}$	$138.9 \pm 5.9^{CD,b}$
5	$188.9 \pm 3.2^{A,cd}$	$157.1 \pm 0.4^{B,de}$	$134.7 \pm 3.0^{C,d}$	$131.5 \pm 1.5^{C,e}$	$135.4 \pm 2.4^{C,b}$
6	$186.8 \pm 5.5^{A,cd}$	$153.2 \pm 0.5^{B,ef}$	$132.5 \pm 3.5^{C,d}$	$130.4 \pm 1.0^{C,e}$	$136.2 \pm 5.2^{C,b}$
7	$183.8 \pm 3.9^{A,d}$	$151.2 \pm 1.5^{B,fg}$	$131.3 \pm 2.5^{C,d}$	$129.3 \pm 0.5^{C,e}$	$134.1 \pm 2.7^{C,b}$
8	$183.5 \pm 4.4^{A,d}$	$148.6 \pm 0.9^{B,g}$	$130.4 \pm 3.2^{C,d}$	$129.1 \pm 1.3^{C,e}$	$134.7 \pm 4.1^{C,b}$
	PDI				
1	$0.302 \pm 0.015^{A,a}$	$0.302 \pm 0.015^{A,a}$	$0.302 \pm 0.015^{A,a}$	$0.302 \pm 0.015^{A,a}$	$0.302 \pm 0.015^{A,a}$
2	$0.256 \pm 0.009^{A,b}$	$0.256 \pm 0.009^{A,b}$	$0.256 \pm 0.009^{A,b}$	$0.256 \pm 0.009^{A,b}$	$0.256 \pm 0.009^{A,b}$
3	$0.250 \pm 0.008^{A,bc}$	$0.250 \pm 0.008^{A,c}$	$0.250 \pm 0.008^{A,bc}$	$0.250 \pm 0.008^{A,bc}$	$0.250 \pm 0.008^{A,bc}$
4	$0.238 \pm 0.012^{A,bcd}$	$0.238 \pm 0.012^{A,bcd}$	$0.238 \pm 0.012^{A,bcd}$	$0.238 \pm 0.012^{A,bcd}$	$0.238 \pm 0.012^{A,bcd}$
5	$0.236 \pm 0.007^{A,bcd}$	$0.236 \pm 0.007^{A,bcd}$	$0.236 \pm 0.007^{A,bcd}$	$0.236 \pm 0.007^{A,bcd}$	$0.236 \pm 0.007^{A,bcd}$
6	$0.232 \pm 0.013^{A,cd}$	$0.232 \pm 0.013^{A,d}$	$0.232 \pm 0.013^{A,cd}$	$0.232 \pm 0.013^{A,cd}$	$0.232 \pm 0.013^{A,cd}$
7	$0.230 \pm 0.006^{A,cd}$	$0.230 \pm 0.006^{A,d}$	$0.230 \pm 0.006^{A,cd}$	$0.230 \pm 0.006^{A,cd}$	$0.230 \pm 0.006^{A,cd}$
8	$0.221 \pm 0.006^{A,d}$	$0.221 \pm 0.006^{A,d}$	$0.221 \pm 0.006^{A,d}$	$0.221 \pm 0.006^{A,d}$	$0.221 \pm 0.006^{A,d}$
	CI (%)				
1	5.34 ± 0.57	2.26 ± 0.01	2.28 ± 0.01	2.27 ± 0.02	1.70 ± 0.02
2	2.24 ± 0.04	1.13 ± 0.01	-	-	-
3	0.83 ± 0.02	-	-	-	-
4	0.58 ± 0.01	-	-	-	-
5	-	-	-	-	-
6	-	-	-	-	-
7	-	-	-	-	-
8	-	-	-	-	-

Note. Different capital superscript alphabets A, B and C in the same row, while different small superscript alphabets a - d in the same column denote statistical significance ($p < 0.05$). PDI = polydispersity index; CI = creaming index

the surfactant-to-oil ratio increased, the mean droplet size of the nanoemulsion decreased, but the PDI increased (Table 6). At all surfactant-to-oil ratios, Tween 85 and Tween 20 produced nanoemulsion with appreciably higher mean droplet size than Kolliphor® EL and Tween 80, probably due to the ability of Kolliphor® EL and Tween 80 to adsorb at the interface and cover the newly formed droplets more rapidly during droplets disruption before they collide to recoalesce. As shown in Figure 1, it is noted that the irritation potential was remarkably lower in Kolliphor® EL than in Tween 80 at all surfactant-to-oil ratios.

AD patients are associated with a lower sensitization threshold and epidermal defects; hence, avoiding surfactants related to the high irritation potential and cytotoxicity in topical products is advisable. From this perspective, Kolliphor® EL seems more advantageous than Tween 80 for AD management. Considering that Ostwald ripening is prone to happen

Table 6
Effects of types of surfactants and surfactant-to-oil ratio on the mean droplet size and PDI of nanoemulsion

Surfactant-to-oil ratio	Tween 85	Kolliphor® EL	Tween 80	Tween 20
		Mean droplet size (nm)		
1.0:8.0	$200.9 \pm 2.0^{A,a}$	$187.6 \pm 1.0^{B,a}$	$181.0 \pm 0.5^{C,a}$	$188.8 \pm 0.1^{B,a}$
1.5:8.0	$175.6 \pm 1.1^{A,b}$	$164.8 \pm 2.2^{B,b}$	$157.7 \pm 1.0^{C,b}$	$166.3 \pm 1.2^{B,b}$
2.0:8.0	$163.1 \pm 2.0^{A,c}$	$146.1 \pm 1.1^{B,c}$	$138.2 \pm 2.0^{C,c}$	$157.2 \pm 1.1^{D,c}$
2.5:8.0	$148.6 \pm 1.8^{A,d}$	$121.6 \pm 3.2^{B,d}$	$130.0 \pm 1.6^{C,d}$	$144.1 \pm 1.0^{D,d}$
3.0:8.0	$134.0 \pm 1.8^{A,e}$	$114.5 \pm 1.5^{B,e}$	$117.5 \pm 1.3^{C,e}$	$139.8 \pm 0.6^{D,e}$
3.5:8.0	$125.4 \pm 1.6^{A,f}$	$110.5 \pm 0.1^{B,f}$	$111.0 \pm 0.6^{B,f}$	$133.7 \pm 3.3^{C,f}$
4.0:8.0	$135.1 \pm 2.3^{A,e}$	$100.3 \pm 0.9^{B,g}$	$111.3 \pm 3.6^{C,f}$	$125.7 \pm 1.5^{D,g}$
		PDI		
1.0:8.0	$0.136 \pm 0.012^{A,a}$	$0.117 \pm 0.008^{B,a}$	$0.140 \pm 0.008^{AC,a}$	$0.152 \pm 0.010^{C,a}$
1.5:8.0	$0.147 \pm 0.012^{A,a}$	$0.130 \pm 0.010^{B,ab}$	$0.154 \pm 0.010^{AC,a}$	$0.164 \pm 0.008^{C,a}$
2.0:8.0	$0.168 \pm 0.012^{A,b}$	$0.145 \pm 0.009^{B,b}$	$0.198 \pm 0.007^{C,b}$	$0.184 \pm 0.010^{C,b}$
2.5:8.0	$0.197 \pm 0.007^{A,c}$	$0.178 \pm 0.010^{B,c}$	$0.242 \pm 0.007^{C,c}$	$0.194 \pm 0.007^{A,bc}$
3.0:8.0	$0.242 \pm 0.009^{A,d}$	$0.213 \pm 0.011^{B,d}$	$0.262 \pm 0.007^{C,d}$	$0.207 \pm 0.004^{B,cd}$
3.5:8.0	$0.243 \pm 0.003^{A,d}$	$0.225 \pm 0.010^{B,de}$	$0.275 \pm 0.004^{C,de}$	$0.216 \pm 0.007^{B,de}$
4.0:8.0	$0.245 \pm 0.006^{A,d}$	$0.239 \pm 0.009^{AB,e}$	$0.281 \pm 0.008^{C,e}$	$0.228 \pm 0.006^{B,e}$

Note. Different capital superscript alphabets A-C in the same row, while different small superscript alphabets a-g in the same column denote statistical significance ($p < 0.05$). PDI = polydispersity index

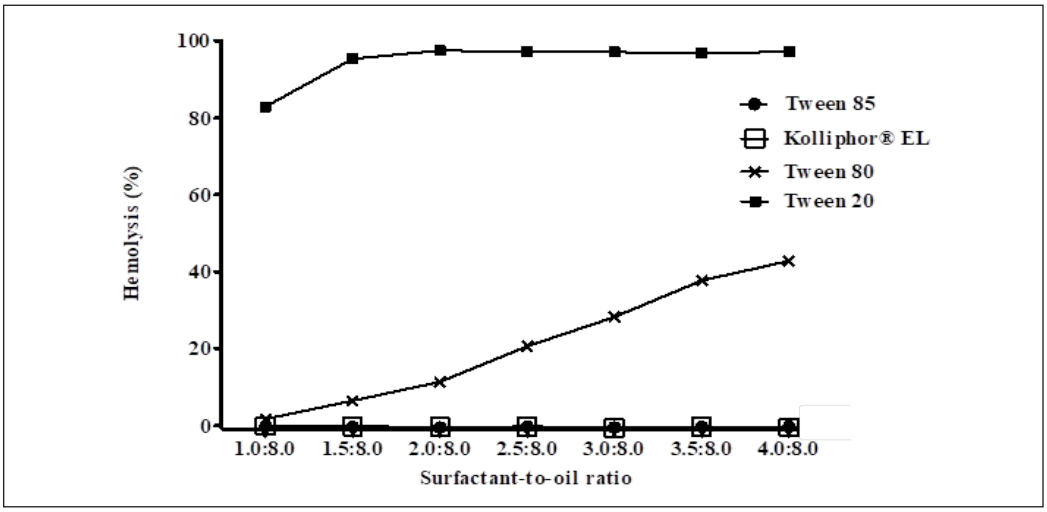

Figure 1. Effect of types of surfactants and surfactant-to-oil ratio on the irritation potential

in highly polydisperse nanoemulsion, it is often ideal for producing nanoemulsion with PDI < 0.200, as narrower size distribution will be more stable against Ostwald ripening. In this context, Kolliphor® EL, at a surfactant-to-oil ratio of 2.5:8.0, which could produce nanoemulsion with small mean droplet size (< 200nm) and PDI < 0.200, was chosen as the optimal nanoemulsion formulation in this study.

Moisturizer Cream Formulation

Physical Stability and Spreadability

The current formulated cream base was composed of a mixture of oil and aqueous phases stabilized by an emulsifier, which is generally inherently unstable and will eventually separate phases. The time needed to show the first sign of instability depends on the oil phase and emulsifier concentrations. Centrifugation is a quick technique to evaluate the physical stability of the formulated products. It was evident that TC02, TC03, TC04, TC07, TC08 and TC12 creams showed signs of physical instability (Table 7), probably due to an insufficient amount of emulsifier to cover the high concentration of oil droplets formed in the creams. Another critical attribute evaluated was spreadability, which refers to the ability of the formulation to spread on the skin.

Overall, the spreadability was decreased with the increments in the oil phase and emulsifying wax concentrations (Table 7). The formulations TC15, TC16, TC18, TC19, and TC20 were semistiff creams, which could influence the patients' compliance as they were not easy to apply. The formulations TC01, TC02 and TC05 were fluid creams, which may result in the uneven spread of the creams and, thus, the dose of antioxidants administered at the application area. The rest of the formulations were classified as semifluid creams, indicating the formulated creams can be spread readily and evenly on the skin during application besides being not too runny to influence the delivery of the correct dose of antioxidants (Chen et al., 2016). Collectively, formulations TC06, TC09, TC10, TC11, TC13, TC14 and TC17 exhibited excellent physical stability and spreadability and were selected for the subsequent evaluations.

Table 7
Physical stability and spreadability of formulated creams

Formulation	Physically unstable upon centrifugation		Spreadability	
	Samples stored at 25°C	Samples stored at 40°C	Spread diameter (cm)	Classification
TC01	*No	No	8.0 ± 0.2[a]	Fluid
TC02	No	*Yes	7.3 ± 0.1[b]	Fluid
TC03	No	Yes	6.9 ± 0.1[c]	Semifluid
TC04	Yes	Yes	6.8 ± 0.1[d]	Semifluid

Table 7 *(continue)*

Formulation	Physically unstable upon centrifugation		Spreadability	
	Samples stored at 25°C	Samples stored at 40°C	Spread diameter (cm)	Classification
TC05	No	No	7.2 ± 0.2^{b}	Fluid
TC06	No	No	6.4 ± 0.3^{e}	Semifluid
TC07	No	Yes	6.1 ± 0.1^{f}	Semifluid
TC08	No	Yes	5.8 ± 0.1^{g}	Semifluid
TC09	No	No	6.8 ± 0.2^{d}	Semifluid
TC10	No	No	6.1 ± 0.1^{f}	Semifluid
TC11	No	No	5.7 ± 0.1^{g}	Semifluid
TC12	No	Yes	5.4 ± 0.2^{h}	Semifluid
TC13	No	No	6.7 ± 0.2^{d}	Semifluid
TC14	No	No	5.8 ± 0.3^{g}	Semifluid
TC15	No	No	5.0 ± 0.1^{i}	Semistiff
TC16	No	No	4.9 ± 0.1^{ij}	Semistiff
TC17	No	No	6.6 ± 0.2^{d}	Semifluid
TC18	No	No	4.9 ± 0.1^{ij}	Semistiff
TC19	No	No	4.8 ± 0.1^{jk}	Semistiff
TC20	No	No	4.7 ± 0.1^{k}	Semistiff

Note. Different superscript alphabets a-k in the same column denote statistical significance ($p < 0.05$). *No indicates that the samples were not physically unstable upon centrifugation at that temperature. *Yes indicates that the samples were physically unstable upon centrifugation at that temperature

Rheological Behaviors

The rheological behaviors analysis was conducted for the selected cream formulations as it provides more detailed information about the cream's physical stability and behaviors during topical application. Figure 2 shows the viscosity flow curve of the TC06, TC09, TC10, TC11, TC13, TC14 and TC17 creams at 25°C, demonstrating that the evaluated creams exhibited shear thinning or pseudoplastic flow behavior (non-Newtonian), a desirable rheological behavior for a topical cream. This observation was corroborated by the calculated flow indices, with values < 1 for all the evaluated creams (Table 8). Looking into more detail on the viscosity profile, under low shear conditions (0.1 s^{-1}), the high viscosity displayed by the formulations contributes to greater retention on the applied skin area for a long-lasting effect and the firmness feel of the creams (Table 8) (Demma et al., 2018). When shear was increased from 0.1 to 100 s^{-1}, a steady decrease in viscosity to < 5 Pa.s, suggesting the easiness of the cream being extruded from a tube and applied over the skin to form a coherent film and covering a large skin area (Krishnaiah et al., 2014), from all the evaluated formulations, it was found that TC11 showed slightly higher viscosity at low (0.1 s^{-1}) and medium (1 s^{-1}) shear rates but relatively lower viscosity at the high

shear rate (100 s^{-1}) and was accompanied by a lower flow index. The consistency index was also calculated, representing the creams' consistency and defining the formulation's effectiveness in inhibiting the repeated collisions of globules in the cream that can promote coalescence and phase separation across time. When compared to other formulations, TC11 demonstrated a slightly higher index value (Table 8). These results suggested that formulation TC11 would possess higher physical stability and ensure good shear-thinning and application attributes on the skin.

Table 8
Apparent viscosity (at low, medium and high shear rates), consistency and flow indices and in vitro occlusion factors of formulated creams

Formulation	Apparent viscosity (Pa.s)			Power law		Occlusion factor (%)
	Shear rate at 0.01 s^{-1}	Shear rate at 1 s^{-1}	Shear rate at 100 s^{-1}	Consistency index (Pa.sn)	Flow index (n)	
TC06	742.6 ± 67.9^{a}	94.9 ± 4.2^{a}	2.0 ± 0.1^{ab}	98.89 ± 4.77^{ab}	0.113 ± 0.006^{ab}	72.15 ± 2.41^{a}
TC09	670.0 ± 42.9^{a}	89.7 ± 5.3^{a}	1.9 ± 0.1^{a}	90.19 ± 4.97^{a}	0.136 ± 0.006^{c}	69.09 ± 2.60^{a}
TC10	788.3 ± 53.7^{ab}	103.2 ± 4.9^{ab}	2.1 ± 0.2^{abc}	102.24 ± 6.17^{b}	0.130 ± 0.012^{cd}	72.41 ± 1.78^{a}
TC11	902.9 ± 81.4^{bc}	118.1 ± 5.9^{bc}	2.2 ± 0.1^{bc}	113.18 ± 3.47^{cd}	0.111 ± 0.004^{a}	79.29 ± 2.30^{b}
TC13	795.4 ± 34.9^{ab}	103.4 ± 3.4^{ab}	2.2 ± 0.1^{bc}	104.57 ± 5.54^{bd}	0.132 ± 0.009^{c}	69.98 ± 1.84^{a}
TC14	998.8 ± 42.0^{c}	127.9 ± 5.5^{c}	2.6 ± 0.1^{d}	116.75 ± 3.80^{c}	0.116 ± 0.001^{abd}	71.64 ± 0.59^{a}
TC17	899.5 ± 86.1^{bc}	113.5 ± 12.7^{bc}	2.3 ± 0.1^{cd}	108.83 ± 5.24^{bcd}	0.127 ± 0.003^{bcd}	70.80 ± 2.19^{a}

Note. Different superscript alphabets a-d in the same column denote statistical significance ($p < 0.05$)

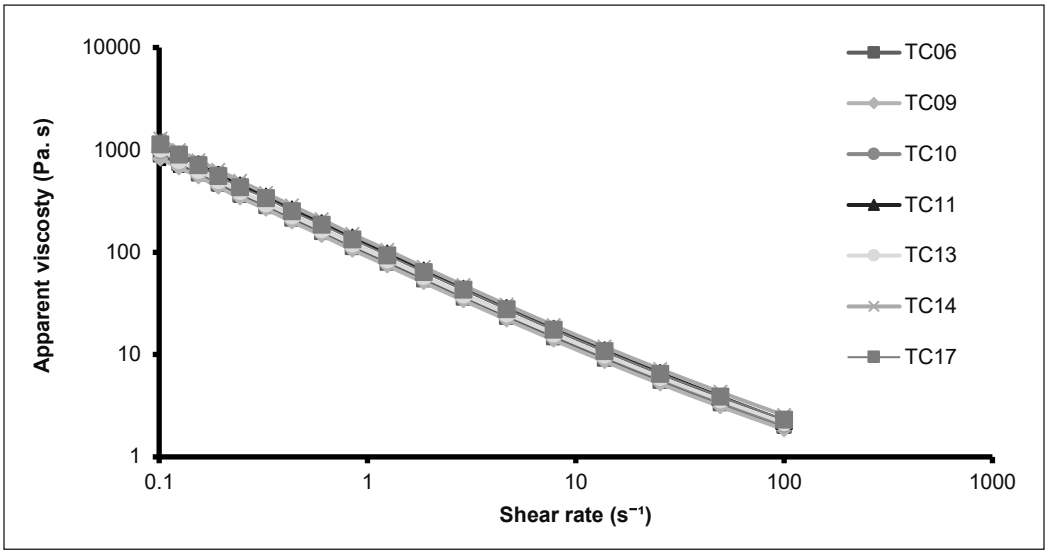

Figure 2. Viscosity flow curves of the formulated creams

In vitro Occlusive

The occlusion effect is one of the critical features of moisturizers to ameliorate AD symptoms via TEWL prevention and skin rehydration (Hebert et al., 2020). Current results demonstrate that the occlusion factor of formulation TC11 was significantly higher than all other formulations (Table 8). It could prevent an additional about 7.14% to 10.2% water loss. The results indicated that applying TC11 could form a thin film to prevent water loss through evaporation, giving greater skin hydration efficiency. The highest concentration of petrolatum and mineral oil incorporated into TC11 and the desirable rheological behaviors exhibited by TC11 would have contributed to this attribute.

Characterization of the Selected Nanoemulsion and Moisturizer Cream Formulations

Morphological Study

A transmission electron microscope is an instrument that allows point-to-point measurement of a single droplet's size of nanoemulsion. The results in Figure 3A showed that the nanoemulsion droplets of the selected formulation were in the nanoscale range with spherical shape and uniform size. It confirms the results obtained from dynamic light scattering measurement (121.5 ± 1.8 nm). These results were similar to those reported by Chong et al. (2018). The microscopic images of the freshly prepared TC11 cream indicate that the moisturizer cream's microstructure was spherical (Figure 3B).

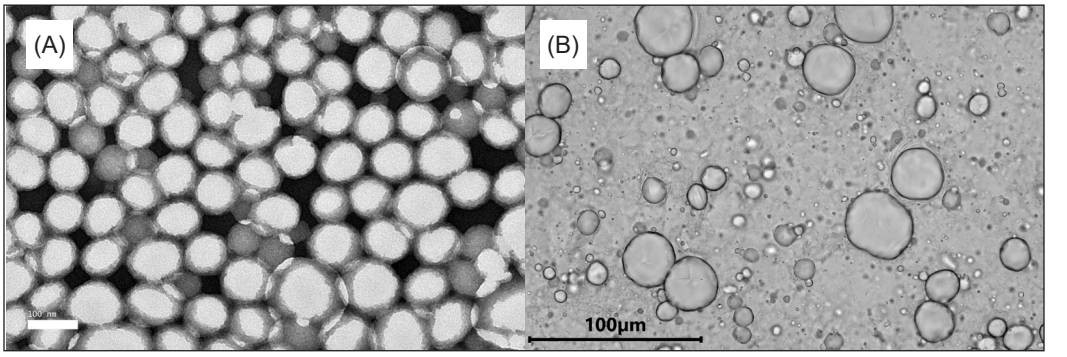

Figure 3. The morphology of the selected (A) nanoemulsion and (B) cream formulations was examined using the transmission electron microscope and light microscope, respectively

In vitro Release

Figure 4 illustrates the antioxidant release profiles for the selected nanoemulsion and cream formulations, showing a concave down-like shape. Within the nanoemulsion matrix, it was observed that the cumulative amount of the released antioxidants per unit of the surface area increased as a function of time until a plateau was attained at 5 hr from the start of the

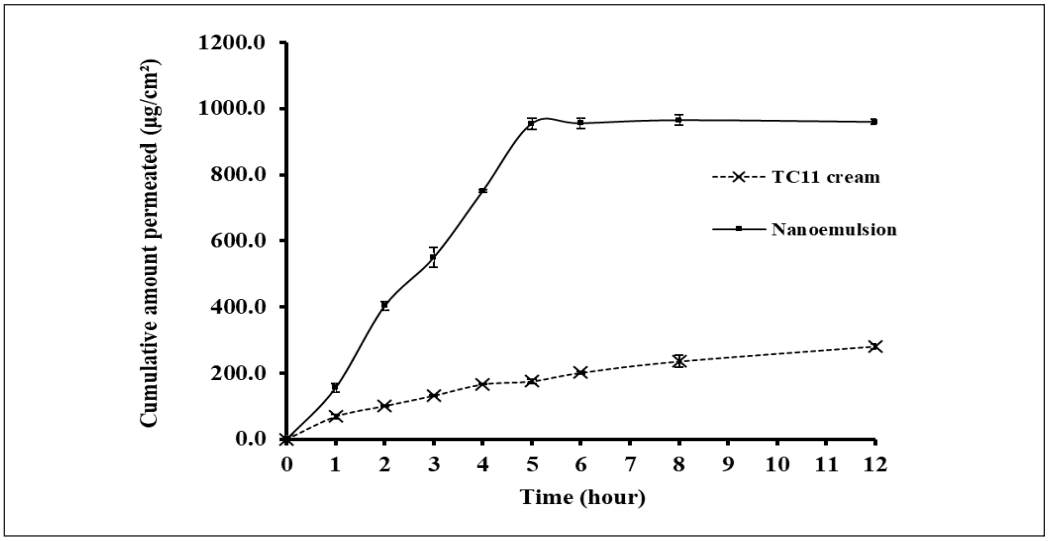

Figure 4. *In vitro* release profiles of encapsulated antioxidants from formulated nanoemulsion and moisturizer cream for 12 hr

analysis. With the TC11 topical cream base matrix, the cumulative amount of the released antioxidants per unit of surface area gradually increased until the end of the investigation. After 12 h, the total release mean percentages of antioxidants were 100% and 30.88% for nanoemulsion and TC11 cream, respectively, evidencing that the cumulative release of antioxidants was greater in nanoemulsion than in TC11 cream. Based on these results, the antioxidants release and diffusion through the membrane could be highly dependent on the delivery matrices or physicochemical properties of the formulation, with the slow release of antioxidants from TC11 cream probably due to the gelling attribute of the carbomer 940 and high viscosity of the cream base. The results were then fitted to the release kinetic models to give an idea of the release rate and mechanisms of antioxidants if used in topical application for the nanoemulsion and when the nanoemulsion was incorporated into the TC11 cream base. The results of the r^2, Akaike information criterion (AIC) and the corresponding constant values for each studied model were summarised in Table 9. Usually, the best-fit model can be identified based on the r^2, and if more than one model is accepted, the best-fit model can be further determined using AIC with the smallest value (Heredia et al., 2022).

Correspondingly, it was observed that the antioxidants released for nanoemulsion have a better adjustment to the zero-order model based on the calculated r^2 value, indicating the release mechanism is independent of the initial concentration of antioxidants but as a function of time only. On the other hand, the TC11 cream base with a slower antioxidant release can fit with Higuchi, Korsmeyer-Peppas and Weibull models based on similar r^2 values. Still, the Korsmeyer-Peppas and Weibull models were the best-fit models identified through AIC. With the β more than one in the Weibull model, the shape of the curve may

probably follow a sigmoidal form during release (Jahromi et al., 2020). Concurrently, the *n* value was located between 0.5 and 1.0 in the Korsmeyer-Peppas model, further suggesting that the release mechanism from the TC11 cream base might be following an anomalous non-Fickian transport (Paarakh et al., 2018).

Table 9
In vitro*, release kinetic study for the antioxidants released from formulated nanoemulsion and moisturizer cream*

Model	Nanoemulsion	Cream
Zero-order		
r^2	0.9989	0.9466
AIC	121.09	1377.27
k_0	19.788	3.189
First-order		
r^2	0.9493	0.9401
AIC	4.04	4.00
k_1	4.734	4.552
Higuchi		
r^2	0.9587	0.9982
AIC	4454.08	51.04
k_H	37.121	8.843
Korsmeyer-Peppas		
r^2	0.9898	0.9943
AIC	4.02	4.01
k_r	0.094	-0.053
n	1.102	0.580
Weibull		
r^2	0.8647	0.9958
AIC	12.79	4.06
$\propto$	0.138	0.079
β	2.0859	0.6361

Note. AIC = Akaike information criterion; r^2 = Coefficient of determination; k_0 = the rate constant of zero-order release kinetics; k_1 = the rate constant of first-order release kinetics; k_H = Higuchi dissolution constant; $\propto$ - scale parameter that defines the timescale of the process; β = curve shape factor

CONCLUSION

Using factorial design methodology, the present study successfully formulated nanoemulsion and moisturizer cream containing TRF, AT and carotenes. The ideal formulation and fabrication conditions of nanoemulsion were successfully screened. The preferred homogenization speed, time and temperature for coarse emulsion preparation using a high-shear mixer were 7000 rpm, 10 min and 45°C, respectively. The optimized homogenization pressure and cycles of high-pressure homogenizer for nanoemulsion formation were 750 bar and five cycles, respectively. The ideal formulation contains 73.75% w/w deionized water, 20% w/w red palm oil and 6.25% w/w Kolliphor® EL. When processed using the abovementioned conditions, nanoemulsion with mean droplet size between 100 to 200 nm and uniform size distribution (PDI < 0.200) was formed. Meanwhile, the moisturizer cream formulation showed that the ideal formulation consisted of 66.8% w/w deionized water, 10% w/w formulated nanoemulsion, 7.5% w/w petrolatum, 7.5% w/w mineral oil, 5% w/w glycerol, 3% w/w emulsifying wax and 0.2% w/w carbomer 940, with a final concentration of 0.1% w/w TRF, 0.1% w/w AT and 0.01% w/w carotenes. This optimally formulated cream could display the preferred shear-thinning behavior during topical application, increase skin hydration with its high occlusion factor, and exhibit Korsmeyer-Peppas and Weibull release kinetic mechanisms during in vitro release.

ACKNOWLEDGEMENTS

This study was supported by the Fundamental Research Grant Scheme (FRGS), Ministry of Higher Education Malaysia, under grant number FRGS/1/2017/STG05/UPM/01/6. The authors wish to express sincere appreciation to Shimadzu Malaysia Sdn. Bhd. for the HPLC instruments and technical assistance provided, which contributed to the success of this project.

REFERENCES

Amin, M. N., Liza, K. F., Sarwar, Md. S., Ahmed, J., Adnan, Md. T., Chowdhury, M. I., Hossain, M. Z., & Islam, M. S. (2015). Effect of lipid peroxidation, antioxidants, macro minerals and trace elements on eczema. *Archives of Dermatological Research*, *307*(7), 617–623. https://doi.org/10.1007/s00403-015-1570-2

Babaye-Nazhad, S., Amirnia, M., Khodaeyani, E., Afza, P. N., Alikhah, H., & Naghavi-Behzad, M. (2013). Effect of oral vitamin E on atopic dermatitis. *Journal of Clinical Research & Governance*, *2*, 66–69. https://doi.org/10.13183/jcrg.v2i2.55

Bruschi, M. (2015). Mathematical models of drug release. In M. Bruschi (Eds.), *Strategies to modify the drug release from pharmaceutical systems* (pp. 63–86). Wood head Publishing. https://doi.org/10.1016/B978-0-08-100092-2.00005-9

Chellapa, P., Mohamed, A. T., Keleb, E. I., Elmahgoubi, A., Eid, A. M., Issa, Y. S., & Elmarzugi, N. A. (2015). Nanoemulsion and nanoemulgel as a topical formulation. *IOSR Journal of Pharmacy*, *5*(10), 43–47.

Chen, M. X., Alexander, K. S., & Baki, G. (2016). Formulation and evaluation of antibacterial creams and gels containing metal ions for topical application. *Journal of Pharmaceutics*, *2016*(1), 5754349. https://doi.org/10.1155/2016/5754349

Chong, W.-T., Tan, C.-P., Cheah, Y.-K., Lajis, A. F., Dian, N. L. H. M., Sivaruby, K., & Lai, O.-M. (2018). Optimization of process parameters in preparation of tocotrienol-rich red palm oil-based anoemulsion stabilized by Tween 80-Span 80 using response surface methodology. *PLoS ONE, 13*(8), e0202771. https://doi.org/10.1371/journal.pone.0202771

Dantas, M. G. B., Reis, S. A. G. B., Damasceno, C. M. D., Rolim, L. A., Rolim-Neto, P. J., Carvalho, F. O., Quintans-Junior, L. J., & Da Silva Almeida, J. R. G. (2016). Development and evaluation of stability of a gel formulation containing the monoterpene borneol. *The Scientific World Journal*, *2016*(1), 7394685. https://doi.org/10.1155/2016/7394685

De Pascale, M. C., Bassi, A. M., Patrone, V., Villacorta, L., Azzi, A., & Zingg, J.-M. (2006). Increased expression of transglutaminase-1 and PPARγ after vitamin E treatment in human keratinocytes. *Archives of Biochemistry and Biophysics*, *447*(2), 97–106. https://doi.org/10.1016/j.abb.2006.02.002

Demma, A., Sartor, F., Tontini, G., Pastorelli, L., & Vecchi, M. (2018). Rheological characterization of two different suspension formulations of beclomethasone dipropionate enemas for rectal administration. *Journal of Pharmaceutical Technology and Drug Research*, *7*, 1. https://doi.org/10.7243/2050-120X-7-1

Galvão, K. C. S., Vicente, A. A., & Sobral, P. J. A. (2018). Development, characterization, and stability of o/w pepper nanoemulsions produced by high-pressure homogenization. *Food and Bioprocess Technology*, *11*(2), 355–367. https://doi.org/10.1007/s11947-017-2016-y

Hayashi, D., Sugaya, H., Ohkoshi, T., Sekizawa, K., Takatsu, H., Shinkai, T., & Urano, S. (2012). Vitamin E improves biochemical indices associated with symptoms of atopic dermatitis-like inflammation in nc/nga mice. *Journal of Nutritional Science and Vitaminology*, *58*(3), 161–168. https://doi.org/10.3177/jnsv.58.161

Hebert, A. A., Rippke, F., Weber, T. M., & Nicol, N. H. (2020). Efficacy of nonprescription moisturizers for atopic dermatitis: An updated review of clinical evidence. *American Journal of Clinical Dermatology*, *21*(5), 641–655. https://doi.org/10.1007/s40257-020-00529-9

Hemrajani, C., Negi, P., Parashar, A., Gupta, G., Jha, N. K., Singh, S. K., Chellappan, D. K., & Dua, K. (2022). Overcoming drug delivery barriers and challenges in topical therapy of atopic dermatitis: A nanotechnological perspective. *Biomedicine & Pharmacotherapy*, *147*, 112633. https://doi.org/10.1016/j.biopha.2022.112633

Heredia, N. S., Vizuete, K., Flores-Calero, M., V, K. P., Pilaquinga, F., Kumar, B., & Debut, A. (2022). Comparative statistical analysis of the release kinetics models for nanoprecipitated drug delivery systems based on poly (lactic-co-glycolic acid). *PLOS ONE*, *17*(3), e0264825. https://doi.org/10.1371/journal.pone.0264825

Hiragun, M., Hiragun, T., Oseto, I., Uchida, K., Yanase, Y., Tanaka, A., Okame, T., Ishikawa, S., Mihara, S., & Hide, M. (2016). Oral administration of β-carotene or lycopene prevents atopic dermatitis-like dermatitis in HR-1 mice. *The Journal of Dermatology*, *43*(10), 1188–1192. https://doi.org/10.1111/1346-8138.13350

Jafari, S. M, Assadpoor, E., He, Y., & Bhandari, B. (2008). Re-coalescence of emulsion droplets during high-energy emulsification. *Food Hydrocolloid*, *22*(7), 1191-1202. https://doi.org/10.1016/j.foodhyd.2007.09.006

Jaffary, F., Faghihi, G., Mokhtarian, A., & Hosseini, S. M. (2015). Effects of oral vitamin E on treatment of atopic dermatitis: A randomized controlled trial. *Journal of Research in Medical Sciences*, *20*(11), 1053. https://doi.org/10.4103/1735-1995.172815

Jahromi, L. P., Ghazali, M., Ashrafi, H., & Azadi, A. (2020). A comparison of models for the analysis of the kinetics of drug release from PLGA-based nanoparticles. *Heliyon*, *6*(2), e03451. https://doi.org/10.1016/j.heliyon.2020.e03451

Javanbakht, M. H., Keshavarz, S. A., Djalali, M., Siassi, F., Eshraghian, M. R., Firooz, A., Seirafi, H., Ehsani, A. H., Chamari, M., & Mirshafiey, A. (2011). Randomized controlled trial using vitamins E and D supplementation in atopic dermatitis. *Journal of Dermatological Treatment*, *22*(3), 144–150. https://doi.org/10.3109/09546630903578566

Ji, H., & Li, X.-K. (2016). Oxidative stress in atopic dermatitis. *Oxidative Medicine and Cellular Longevity*, *2016*(1), 2721469. https://doi.org/10.1155/2016/2721469

Jung, Y. J., Yoon, J.-H., Kang, N. G., Park, S. G., & Jeong, S. H. (2012). Diffusion properties of different compounds across various synthetic membranes using Franz-type diffusion cells. *Journal of Pharmaceutical Investigation*, *42*(5), 271–277. https://doi.org/10.1007/s40005-012-0040-5

Kake, T., Imai, M., & Takahashi, N. (2019). Effects of β-carotene on oxazolone-induced atopic dermatitis in hairless mice. *Experimental Dermatology*, *28*(9), 1044–1050. https://doi.org/10.1111/exd.14003

Kapun, A. P., Salobir, J., Levart, A., Kalcher, G. T., Svete, A. N., & Kotnik, T. (2014). Vitamin E supplementation in canine atopic dermatitis: Improvement of clinical signs and effects on oxidative stress markers. *Veterinary Record*, *175*(22), 560–560. https://doi.org/10.1136/vr.102547

Kato, E., & Takahashi, N. (2012). Improvement by sodium dl-α-tocopheryl-6-O-phosphate treatment of moisture-retaining ability in stratum corneum through increased ceramide levels. *Bioorganic & Medicinal Chemistry*, *20*(12), 3837–3842. https://doi.org/10.1016/j.bmc.2012.04.029

Kim, K. P., Shin, K.-O., Park, K., Yun, H. J., Mann, S., Lee, Y. M., & Cho, Y. (2015). Vitamin c stimulates epidermal ceramide production by regulating its metabolic enzymes. *Biomolecules & Therapeutics*, *23*(6), 525–530. https://doi.org/10.4062/biomolther.2015.044

Krishnaiah, Y. S. R., Xu, X., Rahman, Z., Yang, Y., Katragadda, U., Lionberger, R., Peters, J. R., Uhl, K., & Khan, M. A. (2014). Development of performance matrix for generic product equivalence of acyclovir topical creams. *International Journal of Pharmaceutics*, *475*(1), 110–122. https://doi.org/10.1016/j.ijpharm.2014.07.034

Kruszewski, B., Zawada, K., & Karpiński, P. (2021). Impact of high-pressure homogenization parameters on physicochemical characteristics, bioactive compounds content, and antioxidant capacity of blackcurrant juice. *Molecules*, *26*(6), 1802. https://doi.org/10.3390/molecules26061802

Kuhn, K. R., & Cunha, R. L. (2012). Flaxseed oil – whey protein isolate emulsions: Effect of high-pressure homogenization. *Journal of Food Engineering, 111*(2), 449-457. https://doi.org/10.1016/j.jfoodeng.2012.01.016

Laughter, M. R., Maymone, M. B. C., Mashayekhi, S., Arents, B. W. M., Karimkhani, C., Langan, S. M., Dellavalle, R. P., & Flohr, C. (2021). The global burden of atopic dermatitis: Lessons from the global burden of disease study 1990–2017*. *British Journal of Dermatology*, *184*(2), 304–309. https://doi.org/10.1111/bjd.19580

Lee, J. H., Jeon, Y.-J., Choi, J. H., Kim, H. Y., & Kim, T.-Y. (2017). Effects of vitabridc[12] on skin inflammation. *Annals of Dermatology*, *29*(5), 548–558. https://doi.org/10.5021/ad.2017.29.5.548

Leveque, N., Robin, S., Muret, P., Mac-Mary, S., Makki, S., & Humbert, P. (2003). High iron and low ascorbic acid concentrations in the dermis of atopic dermatitis patients. *Dermatology*, *207*(3), 261–264. https://doi.org/10.1159/000073087

Myriam, M., Sabatier, M., Steiling, H., & Williamson, G. (2006). Skin bioavailability of dietary vitamin E, carotenoids, polyphenols, vitamin C, zinc and selenium. *British Journal of Nutrition*, *96*(2), 227–238. https://doi.org/10.1079/BJN20061817

Oladimeji, F. A., Akinkunmi, E. O., Raheem, A. I., Abiodun, G. O., & Bankole, V. O. (2015). Evaluation of topical antimicrobial ointment formulations of essential oil of *Lippia multiflora* moldenke. *African Journal of Traditional, Complementary and Alternative Medicines*, *12*(5), 135-144. https://doi.org/10.4314/ajtcam.v12i5.18

Paarakh, M. P., Jose, P. A., Setty, C., & Christoper, G. V. P. (2018). Release kinetics – concepts and applications. *International Journal of Pharmacy Research & Technology (IJPRT)*, *8*(1), 12-20. https://doi.org/10.31838/ijprt/08.01.02

Packer, L., Weber, S. U., & Rimbach, G. (2001). Molecular aspects of α-tocotrienol antioxidant action and cell signalling. *The Journal of Nutrition*, *131*(2), 369S-373S. https://doi.org/10.1093/jn/131.2.369S

Parish, W. E., Read, J., & Paterson, S. E. (2005). Changes in basal cell mitosis and transepidermal water loss in skin cultures treated with vitamins C and E. *Experimental Dermatology*, *14*(9), 684–691. https://doi.org/10.1111/j.0906-6705.2005.00340.x

Pasonen-Seppänen, S., Suhonen, M. T., Kirjavainen, M., Suihko, E., Urtti, A., Miettinen, M., Hyttinen, M., Tammi, M., & Tammi, R. (2001). Vitamin C enhances differentiation of a continuous keratinocyte cell line (REK) into epidermis with normal stratum corneum ultrastructure and functional permeability barrier. *Histochemistry and Cell Biology*, *116*(4), 287–297. https://doi.org/10.1007/s004180100312

Peng, J., Dong, W. J., Li, L., Xu, J. M., Jin, D. J., Xia, X. J., & Liu, Y. L. (2015). Effect of high-pressure homogenization preparation on mean globule size and large-diameter tail of oil-in-water injectable emulsions. *Journal of Food and Drug Analysis, 23*(4), 828-835. https://doi.org/10.1016/j.jfda.2015.04.004

Qian, C., & McClements, D. J. (2011). Formation of nanoemulsions stabilized by model food-grade emulsifiers using high-pressure homogenization: Factors affecting particle size. *Food Hydrocolloid, 25*(5), 1000-1008. https://doi.org/10.1016/j.foodhyd.2010.09.017

Rocha-Filho, P. A., Ferrari, M., Maruno, M., Souza, O., & Gumiero, V. (2017). In vitro and in vivo evaluation of nanoemulsion containing vegetable extracts. *Cosmetics*, *4*(3), 32. https://doi.org/10.3390/cosmetics4030032

Roohinejad, S., Oey, I., Wen, J., Lee, S. J., Everett, D. W., & Burritt, D. J. (2015). Formulation of oil-in-water β-carotene microemulsions: Effect of oil type and fatty acid chain length. *Food Chemistry*, *174*, 270–278. https://doi.org/10.1016/j.foodchem.2014.11.056

Sakai, S., Sugawara, T., & Hirata, T. (2011). Inhibitory effect of dietary carotenoids on dinitrofluorobenzene-induced contact hypersensitivity in mice. *Bioscience, Biotechnology, and Biochemistry*, *75*(5), 1013–1015. https://doi.org/10.1271/bbb.110104

Salamanca, C. H., Barrera-Ocampo, A., Lasso, J. C., Camacho, N., & Yarce, C. J. (2018). Franz diffusion cell approach for pre-formulation characterisation of ketoprofen semi-solid dosage forms. *Pharmaceutics*, *10*(3), 148. https://doi.org/10.3390/pharmaceutics10030148

Sato, Y., Akiyama, H., Suganuma, H., Watanabe, T., Nagaoka, M. H., Inakuma, T., Goda, Y., & Maitani, T. (2004). The feeding of β-carotene down-regulates serum ige levels and inhibits the type i allergic response in mice. *Biological and Pharmaceutical Bulletin*, *27*(7), 978–984. https://doi.org/10.1248/bpb.27.978

Savini, I., Rossi, A., Duranti, G., Avigliano, L., Catani, M. V., & Melino, G. (2002). Characterization of keratinocyte differentiation induced by ascorbic acid: Protein kinase c involvement and vitamin c homeostasis. *Journal of Investigative Dermatology*, *118*(2), 372–379. https://doi.org/10.1046/j.0022-202x.2001.01624.x

Siska, B., Snejdrova, E., Machac, I., Dolecek, P., & Martiska, J. (2019). Contribution to the rheological testing of pharmaceutical semisolids. *Pharmaceutical Development and Technology*, *24*(1), 80–88. https://doi.org/10.1080/10837450.2018.1425432

Sivaranjani, N., Rao, S. V., & Rajeev, G. (2013). Role of reactive oxygen species and antioxidants in atopic dermatitis. *Journal of Clinical and Diagnostic Research, 7*(12), 2683–2685. https://doi.org/10.7860/JCDR/2013/6635.3732

Swarnavalli, G. C. J., Dinakaran, S., & Divya, S. (2016). Preparation and characterization of nanosized Ag/SLN composite and its viability for improved occlusion. *Applied Nanoscience*, *6*(7), 1065–1072. https://doi.org/10.1007/s13204-016-0522-2

Tsuduki, T., Kuriyama, K., Nakagawa, K., & Miyazawa, T. (2013). Tocotrienol (unsaturated vitamin e) suppresses degranulation of mast cells and reduces allergic dermatitis in mice. *Journal of Oleo Science*, *62*(10), 825–834. https://doi.org/10.5650/jos.62.825

Uluata, S., Decker, E. A., & McClements, D. J. (2016). Optimization of nanoemulsion fabrication using microfluidization: Role of surfactant concentration on formation and stability. *Food Biophysics*, *11*(1), 52–59. https://doi.org/10.1007/s11483-015-9416-1

Weber, T. M., Samarin, F., Babcock, M. J., Filbry, A., & Rippke, F. (2015). Steroid-free over-the-counter eczema skin care formulations reduce risk of flare, prolong time to flare, and reduce eczema symptoms in pediatric subjects with atopic dermatitis. *Journal of Drugs in Dermatology*, *14*(5), 478–485.

Williamson, S., Merritt, J., & De Benedetto, A. (2020). Atopic dermatitis in the elderly: A review of clinical and pathophysiological hallmarks. *British Journal of Dermatology*, *182*(1), 47–54. https://doi.org/10.1111/bjd.17896

Yarce, C. J., Pineda, D., Correa, C. E., & Salamanca, C. H. (2016). Relationship between surface properties and in vitro drug release from a compressed matrix containing an amphiphilic polymer material. *Pharmaceuticals*, *9*(3), 34. https://doi.org/10.3390/ph9030034

Ye, M., Duan, H., Yao, L., Fang, Y., Zhang, X., Dong, L., Yang, F., Yang, X., & Pan, W. (2019). A method of elevated temperatures coupled with magnetic stirring to predict real time release from long acting progesterone PLGA microspheres. *Asian Journal of Pharmaceutical Sciences*, *14*(2), 222–232. https://doi.org/10.1016/j.ajps.2018.05.010

Zuuren, E. J. van, Fedorowicz, Z., Christensen, R., Lavrijsen, A. P., & Arents, B. W. (2017). Emollients and moisturisers for eczema. *Cochrane Database of Systematic Reviews*, *2*(2). https://doi.org/10.1002/14651858.CD012119.pub2